THE JOURNAL OF PHYSICAL CHEMISTRY Letters

Letter

Cite This: J. Phys. Chem. Lett. 2019, 10, 3426−3432

pubs.acs.org/JPCL

The Simplest Possible Approach for Simulating S_0−S_1 Conical Intersections with DFT/TDDFT: Adding *One* Doubly Excited Configuration

Hung-Hsuan Teh* and Joseph E. Subotnik*

Department of Chemistry, University of Pennsylvania, Philadelphia, Pennsylvania 19104-6323, United States

Supporting Information

ABSTRACT: A simple combination of density functional theory/time-dependent density functional theory (DFT/TDDFT) and configuration interaction is presented to fix the incorrect topology of the S_0−S_1 conical intersection (CI) and allow a description of bond making and bond breaking in photoinduced dynamics. The proposed TDDFT-1D method includes one lone optimized doubly excited configuration in addition to the DFT/TDDFT singly excited states within the context of a large configuration interaction Hamiltonian. Results for ethylene and stilbene are provided to demonstrate that this ansatz can yield physically meaningful potential energy surfaces near S_0−S_1 avoided crossings without changing the vertical excitation energies far from the relevant crossings. We also investigate the famous linear water example to show that the algorithm calculates the correct topology of the S_0−S_1 CI and yields the correct geometric phase.

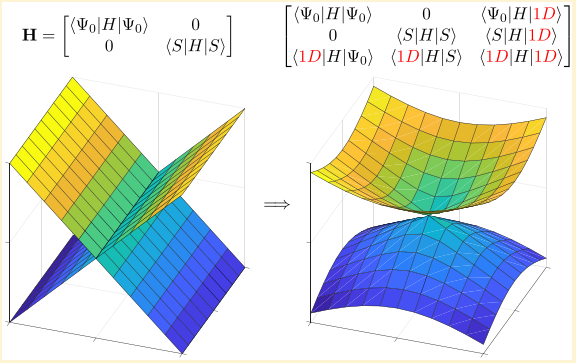

Over the past few decades, conical intersections (CIs) have emerged as crucial points in configuration space as they are now understood to play a key role in many ultrafast and radiationless processes,[1−3] as proven through an increasing number of experimental observations.[4−6] To fully understand chemical dynamics through CIs using computer simulations, precise electronic structure is clearly required: a small change in the potential energy surface can substantially affect dynamical properties.[7] Unfortunately, although powerful approaches are available for small molecular systems, such methods are expensive and often one cannot construct reasonable electronic states for large complex systems, especially near the CIs between the ground state (S_0) and the first excited state (S_1) where static correlation is key and perturbation theory is often impossible. Many widely used approaches yield incorrect descriptions of the S_0−S_1 CI seams, and sometimes even of excited state−excited state seams.[8,9]

Perhaps the most important question about CIs is the dimensionality of the CI branching plane. For a system with N nuclear degrees of freedom (DOF), the CI dimensionality is almost always $N - 2$.[10] For example, a nonlinear water molecule has three nuclear DOF, so the CI dimensionality is one. Thus, if we arbitrarily choose a two-dimensional nuclear subspace, the intersection between the subspace and the CI manifold would be a set of discrete points. If one imagines sitting at a point on the intersection seam, because there are two vectors perpendicular to the CI manifold and one vector normal to the arbitrary two-dimensional nuclear subspace, there will almost always be a total of three independent directions in a three-dimensional nuclear space through which one can break the degeneracy of a CI seam. In other words, a random sampling of a two-dimensional space should imply that all CI points are completely isolated. A similar statement can be made for a linear water molecule: the intersection of the CI manifold with an arbitrary two-dimensional nuclear subspace should be a set of discrete points.

Unfortunately, in spite of these simple formal arguments, approaches like DFT/TDDFT are known to predict incorrect results for the dimensionality of CI seams, as has been explained clearly before.[8,9] Consider a 2 × 2 model Hamiltonian. In order to find a nuclear geometry with a degeneracy, two constraints must be satisfied: both the energy difference and the coupling between the two states must be zero. However, for DFT/TDDFT, just as for Hartree−Fock (HF) and CIS/CIS-inspired methods[11−19] all except CIS(2),[20] the coupling between the ground state and single excitation states is always (by definition) zero according to the Brillouin theorem, so that only one constraint needs to be satisfied to reach a geometry with degenerate states, leading to an incorrect description of the CI topology: the seam now has dimension $N - 1$.

Now, given this grotesque failure of DFT and TDDFT, one might suspect that computational photophysicists and photochemists would seek alternative approaches. However, DFT and TDDFT clearly remain the methods of choice for the vast majority of computational chemists: these methods achieve a

Received: April 5, 2019
Accepted: May 28, 2019
Published: May 28, 2019

DOI: 10.1021/acs.jpclett.9b00981
J. Phys. Chem. Lett. 2019, 10, 3426−3432

nice balance between precision and computational cost and can be remarkably successful as far as simulating electronic structure, energies and geometries included. Furthermore, DFT and TDDFT are often the only possible approaches for analyzing large complex systems and S_0-S_1 derivative couplings are available and widely used today.[21] For this reason, rather than abandon DFT/TDDFT, there is an intense interest nowadays in fixing up the DFT/TDDFT CI problem without altering the DFT/TDDFT potential energy surfaces far from the CI seam.[22,23] Li et al. suggested that one can couple the DFT ground state to a TDDFT single by using the same matrix element as appears in HF-CIS coupling, namely, $(a|f|i)$, only replacing HF orbitals with Kohn−Sham (KS) orbitals.[23] Shu et al. suggested using two different exchange−correlation functionals, one for optimizing KS orbitals and one for constructing the KS Tamm−Dancoff approximation (KS-TDA) matrix, so that now the couplings between the DFT ground state and single excitation states are no longer zero.[22] More generally, although not in the context of conical intersections per se, Grimme and Waletzke long ago fashioned a semiempirical DFT-MRCI algorithm that constructed a heuristic configuration interaction Hamiltonian by choosing references of low energy to treat the static correlation problem in DFT;[24] Kraka developed DFT-GVB;[25] and Gräfenstein and Cremer published some extensions of CAS-DFT.[26] Other approaches for treating static correlation with DFT include REKS,[27] ROKS,[28] and indirectly CDFT-CI.[29] Evangelista et al. have also developed OCDFT which minimizes ground- and excited-state energies variationally over the space of single Slater determinants using one universal functional and within the constraint that the ground and excited states must be orthogonal to each other.[30] As most relevant to our research, Maitra et al. have investigated the possibility of calculating doubly excited-state energies by dressing the linear response matrix as if a single doubly configuration were included in a large configuration interaction Hamiltonian, so that the frequency dependence of the exchange−correlation kernel appears.[31,32] In so doing, they could investigate one single−one double mixing (though crossings with the ground state were not considered). Lastly, if one is prepared to use more eleborate wave function methods, Gagliardi et al.[33] recently developed a multiconfiguration pair-DFT ansatz by which the electron kinetic energy and classical electrostatic energy are calculated from a multiconfiguration self-consistent-field wave function and then combined with a one-shot inclusion of an on-top density functional; this approach should also be able to extract the correct S_0-S_1 topology.

Clearly, from the list above, there is a great deal of interest in understanding avoided crossings to the ground state in the context of DFT/TDDFT. However, even today, propagating nonadiabatic systems forward in time remains difficult with crossings from S_1 to S_0 as there is not yet a consensus on how to achieve a stable and accurate algorithm that is inexpensive enough for ab initio DFT/TDDFT dynamics when multi-reference effects are prevalent.

With this background in mind, in this Letter, we will investigate yet another approach for merging DFT and configuration interaction that we feel combines the best elements of the previous list of algorithms and should be very helpful for simulating S_1 to S_0 dynamical processes insofar as (i) the approach should be able to treat bond-making and breaking (as in ref 33), at least for a single bond; (ii) the cost should be very inexpensive (i.e., roughly the cost of TDDFT alone); and (iii) the approach is simple enough such that analytic gradients and nonadiabatic couplings will be easily achievable so that the algorithm can certainly be applied to photoinduced dynamics (as in ref 23 and 22). Our ansatz is to utilize the fictitious DFT/TDDFT wave functions in the framework of a larger configuration interaction Hamiltonian. The basis for our configuration interaction Hamiltonian includes the ground-state DFT wave function, the set of single excitation states (where one electron excited from an occupied KS spin orbital $\{i\}$ to a KS virtual orbital $\{a\}$), and *one* doubly excited configuration (with a pair of electrons excited from a specific KS spatial orbital h to another specific KS spatial orbital l):

$$\mathbf{H} = \begin{bmatrix} \langle\Psi_0|H|\Psi_0\rangle & 0 & \langle\Psi_0|H|\Psi_{h\bar{h}}^{l\bar{l}}\rangle \\ 0 & \langle\Psi_i^a|H|\Psi_j^b\rangle & \langle\Psi_i^a|H|\Psi_{h\bar{h}}^{l\bar{l}}\rangle \\ \langle\Psi_{h\bar{h}}^{l\bar{l}}|H|\Psi_0\rangle & \langle\Psi_{h\bar{h}}^{l\bar{l}}|H|\Psi_j^b\rangle & \langle\Psi_{h\bar{h}}^{l\bar{l}}|H|\Psi_{h\bar{h}}^{l\bar{l}}\rangle \end{bmatrix} \tag{1}$$

Henceforth, we will denote the Hamiltonian in eq 1 as the CIS-1D or TDDFT-1D Hamiltonian. We will show below that diagonalizing eq 1 yields energies with correct topologies for S_0-S_1 CIs, as illustrated by the famous water molecule example of Levine et al.[9] We will also show that our TDDFT-1D ansatz with KS orbitals does not dramatically change the vertical excitation energies far from the S_0-S_1 CI so that eq 1 should be a strong candidate for simulating both absorption and the subsequent photoinduced dynamics. Finally, before concluding, by using the water molecule as an example, we will also demonstrate that eq 1 is completely consistent with the geometric phase along a path enclosing a CI in the water system (also known as the Berry phase[34,35]).

Theory. To apply configuration interaction as described above, our initial task is to construct one key doubly excited state, and ideally this state should aid us in describing bond breaking. To that end, instead of choosing a double excitation from the highest occupied molecular orbital (HOMO) to the lowest unoccupied molecular orbital (LUMO), we choose to optimize both the occupied molecular orbital (h) and the virtual molecular orbital (l) so as to minimize the energy of the double excitation state $|\Psi_{h\bar{h}}^{l\bar{l}}\rangle$. In a sense, this unique doubly excited state resembles the MOM states as constructed by Gilbert et al.,[36] but with less generality: we relax occupied and virtual orbitals separately, $|h\rangle = \sum_{i=1}^{N_o} c_i|i_0\rangle$ and $|l\rangle = \sum_{a=1}^{N_v} c_a|a_0\rangle$, so that the doubly excited state is strictly orthogonal to the original ground state. The related set of coupled equations (see the Supporting Information for more details) are

$$[f - (2J_h - K_h) + (2J_l - K_l)]|h\rangle = \epsilon_h|h\rangle \tag{2a}$$

$$[f + (2J_h - K_h) - (2J_l - K_l)]|l\rangle = \epsilon_l|l\rangle \tag{2b}$$

Here f stands for the Fock operator, and ϵ_p denotes the pth orbital energy. J_p and K_p represent Coulomb and exchange operators, respectively. When we work with the exact Hamiltonian and a set of HF orbitals, we find that the optimization routine usually requires only a few iterations to converge.

Let us now discuss the construction of the configuration interaction Hamiltonian in more detail. With the optimized

DOI: 10.1021/acs.jpclett.9b00981
J. Phys. Chem. Lett. 2019, 10, 3426−3432

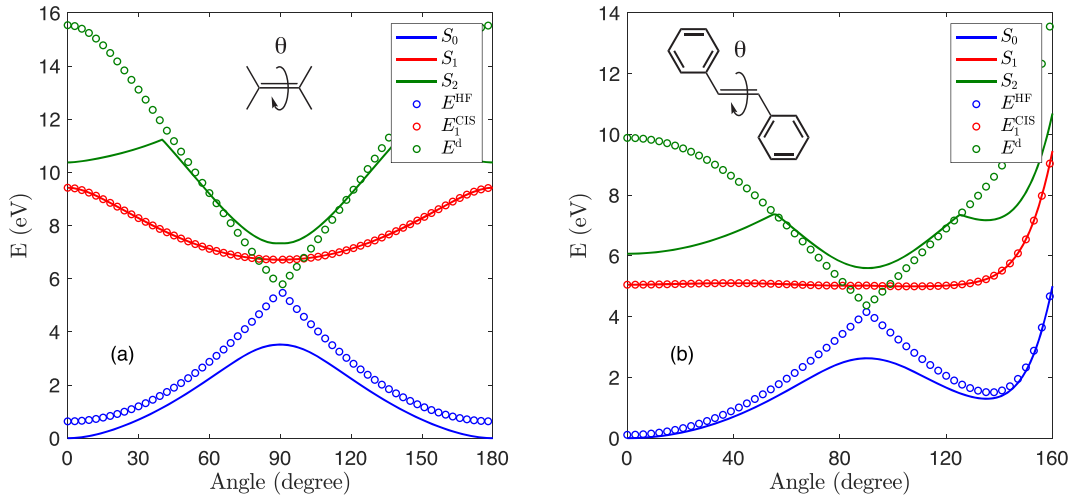

Figure 1. Results of (a) ethylene and (b) stilbene. Blue, red, and green solid lines represent S_0, S_1, and S_2 CIS-1D energies, respectively. The HF ground-state energy (blue circle), the lowest CIS excited-state energy (red circle), and the lone doubly excited-state energy (greeen circle) are also included. Note that, especially for stilbene, the ground-state energy changes strongly only near the S_0−S_1 crossing.

HF orbitals, the elements of the corresponding CIS-1D Hamiltonian H can be calculated as follows:

$$\langle \Psi_0|H|\Psi_0\rangle = E_0^{\mathrm{HF}} \tag{3a}$$

$$\langle \Psi_0|H|S_j^b\rangle = 0 \tag{3b}$$

$$\langle \Psi_0|H|\Psi_{h\bar{h}}^{l\bar{l}}\rangle = (hl|hl) \tag{3c}$$

$$\langle S_i^a|H|S_j^b\rangle = (E_0^{\mathrm{HF}} + \epsilon_a - \epsilon_i)\delta_{ij}\delta_{ab} + 2(jb|ai) - (ji|ab) \tag{3d}$$

$$\langle S_i^a|H|\Psi_{h\bar{h}}^{l\bar{l}}\rangle = \sqrt{2}\,[\delta_{ih}(al|hl) - \delta_{al}(hl|hi)] \tag{3e}$$

$$\langle \Psi_{h\bar{h}}^{l\bar{l}}|H|\Psi_{h\bar{h}}^{l\bar{l}}\rangle = E_0^{\mathrm{HF}} - 2f_{hh} + 2f_{ll} + (ll|ll) + (hh|hh) - 4(hh|ll) + 2(hl|lh) \tag{3f}$$

In eq 3, we work with noncanonical occupied orbitals, chosen such that $\{i, j, ..., h\}$ denote a basis for the occupied space, and $\{a, b, ..., l\}$ denote a basis for the virtual space. $|\Psi_0\rangle$ and E_0^{HF} represent the HF ground state and the corresponding eigenenergy. $|S_i^a\rangle$ is a singlet excited state $(|\Psi_i^a\rangle + |\Psi_{\bar{i}}^{\bar{a}}\rangle)/\sqrt{2}$, and $|\Psi_{h\bar{h}}^{l\bar{l}}\rangle$ is the lone double excitation state with a pair of electrons excited from orbital h to orbital l. Only singlet states are considered in this Letter, but the method can be easily generalized to include triplet states. $(pq|rs)$ stands for the two-electron integral $\int \mathrm{d}\mathbf{r}\,\mathrm{d}\mathbf{r}'\phi_p^*(\mathbf{r})\phi_q(\mathbf{r})\frac{1}{|\mathbf{r}-\mathbf{r}'|}\phi_r^*(\mathbf{r}')\phi_s(\mathbf{r}')$ of the spatial orbitals. The total computational expense for diagonalizing $\mathbf{H}$ in eq 3 is roughly the same as that for a CIS calculation; the same is true for the case of a DFT/TDDFT ansatz with KS orbitals (see below).

Equations 3 (and 4 later) are effectively one approach for performing a CAS-CI calculation, without ever fully optimzing the orbitals as is standard in a true CASSCF calculation[37] (other approaches can be found in refs 38 and 39). By choosing the h and l orbitals variationally at the beginning and then including all single excitations, we might hope for a reasonable set of orbitals (as well as excitation energies and geometries). At the very least, by including the doubly excited state, one automatically goes beyond Brillouin's theorem and recovers the correct dimensionality of an S_0−S_1 CI. Furthermore, the procedure above is conceptually rigorous, insofar as one works with the true Hamiltonian and wave functions, albeit in a reduced subspace. Nevertheless, our starting points are still HF and CIS, which are known to offer very incorrect excitation energies.[17,40,41] To do better, one would like to use DFT/TDDFT instead.[42] After all, DFT is a well-established technique which effectively includes some local correlation energy by ansatz and should be a better starting point.

To apply the configuration interaction framework above to DFT/TDDFT, two assumptions are made here. First, we will treat the KS orbitals (which describe the fictitious system of noninteracting electrons) as real orbitals describing a real system. Very often Kohn−Sham (KS) orbitals mimic HF orbitals at least qualitatively. Second, we construct the TDDFT-1D Hamiltonian with KS orbitals in the following way: by taking the direct coupling (and ignoring all exchange effects) between (i) the ground state and the doubly excited state, as well as between (ii) all the singly excited states and the doubly excited state:

$$\langle \Psi_0|H^{\mathrm{KS}}|\Psi_0\rangle = E^{\mathrm{DFT}} \tag{4a}$$

$$\langle \Psi_0|H^{\mathrm{KS}}|S_j^b\rangle = 0 \tag{4b}$$

$$\langle \Psi_0|H^{\mathrm{KS}}|\Psi_{h\bar{h}}^{l\bar{l}}\rangle = (hl|hl) \tag{4c}$$

$$\langle S_i^a|H^{\mathrm{KS}}|S_j^b\rangle = (E^{\mathrm{DFT}} + \epsilon_a - \epsilon_i)\delta_{ij}\delta_{ab} + 2(jb|ai) + \int \mathrm{d}\mathbf{r}\,\mathrm{d}\mathbf{r}'\phi_j^*(\mathbf{r})\phi_i(\mathbf{r})f_{xc}(\mathbf{r},\mathbf{r}')\phi_a^*(\mathbf{r}')\phi_b(\mathbf{r}') \tag{4d}$$

$$\langle S_i^a|H^{\mathrm{KS}}|\Psi_{h\bar{h}}^{l\bar{l}}\rangle = \sqrt{2}\,[\delta_{ih}(al|hl) - \delta_{al}(hl|hi)] \tag{4e}$$

$$\langle \Psi_{h\bar{h}}^{l\bar{l}}|H^{\mathrm{KS}}|\Psi_{h\bar{h}}^{l\bar{l}}\rangle = 2\sum_{p=1,\cdots,h-1,l}\epsilon_p + 2\sum_{p,q=1,\cdots,h-1,l}(pp|qq) + E_{\mathrm{xc}}[\rho_{\mathrm{d}}] + \int \mathrm{d}\mathbf{r}V_{\mathrm{xc}}(\mathbf{r})\rho_{\mathrm{d}}(\mathbf{r}) \tag{4f}$$

Here we use the same notation as before, but the orbitals are now the optimized Kohn−Sham orbitals (OKSOs) instead of

DOI: 10.1021/acs.jpclett.9b00981
J. Phys. Chem. Lett. 2019, 10, 3426−3432

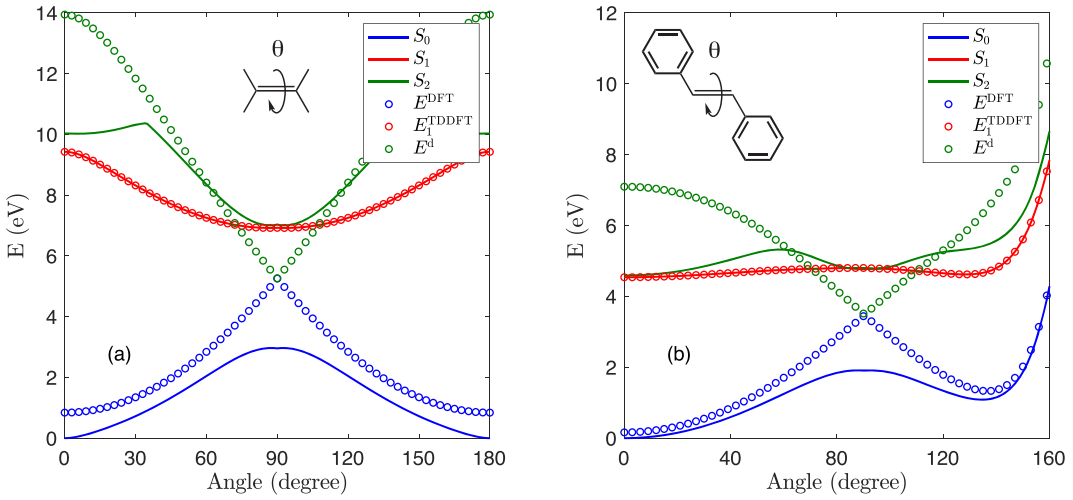

Figure 2. Results of (a) ethylene and (b) stilbene. Blue, red, and green solid lines represent S_0, S_1, and S_2 TDDFT-1D B3LYP energies, respectively. The DFT ground-state energy (red circle), the first TDDFT excited-state energy (blue circle), and the one double excitation state energy (green circle) are also included. Notice again that, especially for stilbene, the ground-state energy does not change very much except near the S_0−S_1 crossing.

the optimized Hartree−Fock orbitals (OHFO). E^{DFT} denotes the DFT energy. $E_{xc}[\rho]$ is the exchange−correlation functional of the electron density ρ, $V_{xc}(\mathbf{r}) = \delta E_{xc}[\rho]/\delta\rho(\mathbf{r})$, and $f_{xc}(\mathbf{r}, \mathbf{r}') = \delta E_{xc}[\rho]/\delta\rho(\mathbf{r})\delta\rho(\mathbf{r}')$ is evaluated at the ground-state density in the static limit.[43,44] ρ_d stands for the electron density corresponding to the double excitation state, with a pair of electrons being excited from orbital h to orbital l.

A few key points should be emphasized here: (i) Equation 4d has exactly the same form as eq 3d except for the fact that the exchange two-electron term has now been replaced with the DFT exchange−correlated functional; eq 4d is the standard linear response tensor for TDDFT within the TDA,[45] which often yields good excitation energies for molecular systems, i.e., better excitation energies than CIS. (ii) For the doubly excited state, the energy is constructed intuitively in the same way as the DFT energy, but with ρ_d as the input. Because we use the raw couplings between the ground state and the single excitation states in eq 3c (as well as between the ground state and the double excitation state in eq 3e), we computationally avoid the dilemma of whether to use ρ and ρ_d when coupling the fictitious KS wave function to the fictitious single/double wave functions. It is possible, however, that in the future we will find it prudent to scale the raw couplings by some empirical factor. (iii) In practice, the optimization of the DFT $|h\rangle$ and $|l\rangle$ orbitals is faster than for the case of the HF orbitals, and the optimization changes the energy less dramatically, confirming the well-known fact that DFT orbitals are more physically meaningful than HF orbitals (see the Supporting Information).

Results: Ethylene and Stilbene. In Figure 1, we plot results for ethylene and stilbene, where we calculate the CIS-1D energies using the OHFOs. S_0, S_1, and S_2 energies are shown in blue, red, and green solid lines, respectively. For comparison, the HF ground-state energy (blue circle), the lowest CIS-state energy (red circle), and the lone doubly excited-state energy (green circle) are also plotted. Note that the CIS-1D S_1 energy is superimposed with the lowest CIS excited-state energy, from which we must conclude that the coupling between the single excitation states and the lone double excitation state is weak. The most important feature to notice in Figure 1 is that inclusion of the lone double lowers the S_0 energy at the crossing for both ethylene and stilbene, but the effect is not large far from the S_0−S_1 crossing; this statement is true especially for stilbene. In this sense, the CIS-1D method will rely on the fact that truncated configuration interaction methods with doubles are not size-consistent: the energy correction does not grow linearly with the system size. As such, the correction should be large only when there is a possibility of strong static correlation, e.g. as we expect at an avoided crossing when two configurations have large occupation. In general, one hopes that the effect of including a double will be apparent only near an S_0−S_1 crossing for larger and larger molecules (with larger and larger configuration interaction Hamiltonians).

Now, the hope of the present method is that with better orbitals and a better treatment of short-range interaction, TDDFT-1D can perform even better than CIS-1D for systems with rich photophysics, such as ethylene and stilbene. To that end, in Figure 2, we present B3LYP results for ethylene and stilbene for the exact same geometries and offer both accurate energies as well as good crossing geometries. Notice that the potential energy surface around $\theta = \pi/2$ for S_0 is still reasonably smooth (there are tiny drops in energy on the order of 0.01 eV very close to $\theta = \pi/2$), which should allow for TDDFT-1D dynamics. Equally important, notice again that, compared with DFT/TDDFT results, TDDFT-1D excitation energies do not change much far from the crossing at $\theta = \pi/2$, especially for the larger stilbene system. Again, the same argument about size inconsistency as discussed above applies here. Altogether, this set of data suggests that a TDDFT-1D approach has the strong potential to allow for nonadiabatic simulations of photochemical dynamics with S_1 to S_2 transitions, while retaining the successes of DFT/TDDFT as far as simulating experimental absorption spectra. Obviously, a great deal of further benchmarking will be necessary to strengthen and/or confirm this prediction.

Dimensionality of the CI Branching Plane. Having investigated S_0−S_1 crossings, we next focus our attention to the topology of a S_0−S_1 CI. We focus on the famous water example as studied by Levine et al.[9] We fix one oxygen atom and one hydrogen

DOI: 10.1021/acs.jpclett.9b00981
J. Phys. Chem. Lett. 2019, 10, 3426−3432

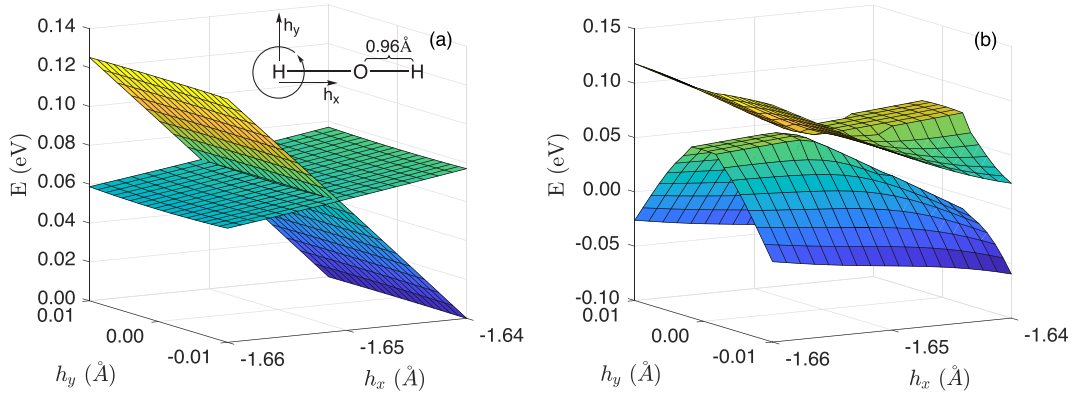

Figure 3. Results for the water molecule with (a) a DFT/TDDFT calculation and (b) a CIS-1D with OKSO. Notice that on the left, the S_0−S_1 crossing is a line, whereas, on the right, one finds the correct conical topology for the S_0−S_1 CI.

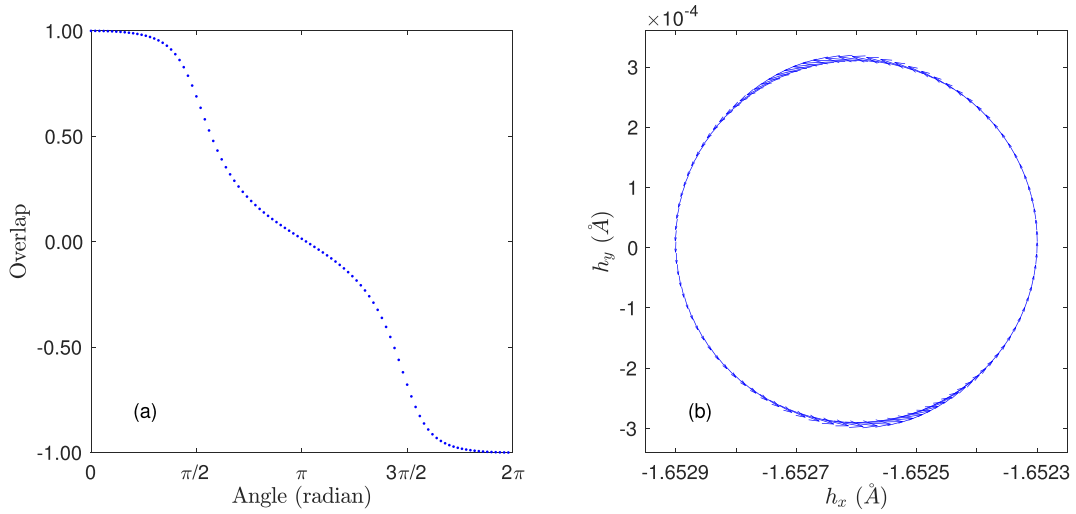

Figure 4. Results of the water molecule. (a) The overlap of the wave function between (i) the initial point (with angle $\theta = 0$) and (ii) all other points along the circle trajectory ($0 < \theta \leq 2\pi$). (b) The derivative coupling along the circle path has the correct structure as one would expect for a linear coupling Hamiltonian with a CI at $x = y = 0$.

atom with a distance 0.96 Å between them and displace the second hydrogen atom in a two-dimensional plane with coordinates (h_x,h_y). For both linear and nonlinear water molecules, within an arbitrary two-dimensional nuclear subspace, the CI manifold should be just a set of discrete points. However, as shown in Figure 3a and ref 9, DFT/TDDFT calculations predict a linear intersection as found by Levine et al.[9] Moreover, the DFT energy is larger than the TDDFT energy for $h_x > -1.650$ Å. By comparison, as shown in Figure 3b, TDDFT-1D shows the correct topology: the putative CI is at (−1.6526, 0) with an energy gap less than 0.001 eV in this case. (Converging the electronic structure exactly on the line $(h_x, 0)$ is difficult with DFT/TDDFT, but DFT is stable and the algorithm converges with even the smallest displacement from $y = 0$.)

Finally, to verify that the putative CI in Figure 3 is truly a CI, we investigate whether there would be a sign change (i.e., geometric phase) for the electronic wave function as one traverses a closed path rounding the putative CI in Figure 3. The geometric phase γ is evaluated by integrating the derivative coupling $\mathbf{d}_{01}(\mathbf{R}) \equiv \langle \Psi_0(\mathbf{R})|\nabla_{\mathbf{R}}|\Psi_1(\mathbf{R})\rangle$ along a trajectory C enclosing the CI

$$\gamma \simeq \oint_C \mathbf{d}_{01}\cdot d\mathbf{R} \tag{5}$$

We move one of the hydrogen atoms around in a circular trajectory surrounding the crossing for a set of different radii (results shown in Figure 4, set radius as 3×10^{-4} Å). At each point on the trajectory, the derivative coupling is evaluated by utilizing the finite difference method (a step size of 5×10^{-6} Å is used). Because for a real Hamiltonian there are only two choices for each eigenstates (+ or −), we use the condition $\langle \Psi_i(\mathbf{R} + d\mathbf{R})|\Psi_i(\mathbf{R})\rangle \sim 1$ to fix the phase of each wave function of each point assuming the distance dR between two points along the path is small. (Indeed, an arbitrary phase $e^{i\gamma'(\mathbf{R})}$ on top of the wave function does not change the topological invariance of γ;[34] therefore, we can consider only the real eigenstates of H, and enforcing continuity of the wave function along a path is obvious.) After the alignment, we can investigate the overlap between the electronic ground state at the starting point $|\Psi_0(\mathbf{r}_i)\rangle$ and all other points. We observe that $\langle \Psi_0(\mathbf{r}_i)|\Psi_0(\mathbf{r}_f)\rangle \sim -1$ (the subscripts i and f represent initial and final, respectively) as shown in Figure 4a, proving that there are odd numbers of CIs enclosed within the circle path (while also demonstrating that one can ignore the effect of S_2 or higher electronic states on the S_0−S_1 CI). The two-

DOI: 10.1021/acs.jpclett.9b00981
J. Phys. Chem. Lett. 2019, 10, 3426−3432

dimensional derivative coupling results are provided in Figure 4b, and the corresponding numerical value of the geometric phase by evaluating the line integral along the path is 3.1415, which confirms that an odd number of CIs exist within the circle path.

Conclusions. Guided by a desire (i) to allow for breaking a single bond while also (ii) fixing the failure of DFT/TDDFT to recover the correct S_0−S_1 topology, we have introduced a simple configuration interaction scheme incorporating the fictitious DFT and TDDFT wave function into a slightly larger effective Hamiltonian; this TDDFT-1D effective Hamiltonian includes one lone double excitation state, $|\Psi^{l\bar{l}}_{h\bar{h}}\rangle$, where h and l are chosen variationally, but so far, in practice, they are close to the HOMO and LUMO wave functions. With such a simple ansatz, one can effectively recover a simple CAS-CI(2,2) wave function where the active orbitals are the HOMO and LUMO, and by including the set of single excitations, ideally one would hope that results will be not far from MRCIS results.[46] Furthermore, one should be able to model breaking and making a single shared electronic bond while ideally keeping the accuracy of DFT/TDDFT excitation energies. Lastly, by diagonalizing the TDDFT-1D Hamiltonian, one can also recover the correct S_0−S_1 topology, so that photochemical dynamics should be describable with this method. Overall, while TDDFT-1D will certainly not be as general or accurate as other modern approaches for merging DFT pair correlation energies with CAS wave functions,[33] and we have not attempted to justify our use of TDDFT wave functions or demonstrated that we do not double-count energies, our instinct is that adding a lone double can provide an inexpensive balance between CAS(2,2) avoided crossing topologies and vertical DFT/TDDFT excitation energies (that are accurate enough). Only time will tell. Given our outstanding goal of simulating photochemical dynamics, the next step forward will be to build gradients and derivative couplings (which should be straightforward to extract by design) and assess the performance of this CIS-1D/TDDFT-1D formalism.

■ ASSOCIATED CONTENT

Supporting Information

The Supporting Information is available free of charge on the ACS Publications website at DOI: 10.1021/acs.jpclett.9b00981.

Derivation of eq 2 and description of how to solve for the lone doubly excited state (PDF)

■ AUTHOR INFORMATION

Corresponding Authors

*E-mail: teh@sas.upenn.edu.

*E-mail: subotnik@sas.upenn.edu.

ORCID

Hung-Hsuan Teh: 0000-0002-6485-5767

Notes

The authors declare no competing financial interest.

■ ACKNOWLEDGMENTS

This material is based upon work supported by the Air Force Office of Scientific Research (AFOSR) under Award Numbers AFOSR FA9550-18-1-0420 and AFOSR FA9550-18-1-0497. J.E.S. thanks Todd Martinez for a series of very helpful conversations.

■ REFERENCES

(1) Schuurman, M. S.; Stolow, A. Dynamics at Conical Intersections. *Annu. Rev. Phys. Chem.* **2018**, *69*, 427.

(2) Zhu, X.; Yarkony, D. R. Non-Adiabaticity: The Importance of Conical Intersections. *Mol. Phys.* **2016**, *114*, 1983.

(3) Matsika, S.; Krause, P. Nonadiabatic Events and Conical Intersections. *Annu. Rev. Phys. Chem.* **2011**, *62*, 621.

(4) Musser, A. J.; Liebel, M.; Schnedermann, C.; Wende, T.; Kehoe, T. B.; Rao, A.; Kukura, P. Evidence for Conical Intersection Dynamics Mediating Ultrafast Singlet Exciton Fission. *Nat. Phys.* **2015**, *11*, 352.

(5) Wörner, H. J.; Bertrand, J. B.; Fabre, B.; Higuet, J.; Ruf, H.; Dubrouil, A.; Patchkovskii, S.; Spanner, M.; Mairesse, Y.; Blanchet, V.; Mével, E.; Constant, E.; Corkum, P. B.; Villeneuve, D. M. Conical Intersection Dynamics in NO_2Probed by Homodyne High-Harmonic Spectroscopy. *Science* **2011**, *334*, 208.

(6) Polli, D.; Altoè, P.; Weingart, O.; Spillane, K. M.; Manzoni, C.; Brida, D.; Tomasello, G.; Orlandi, G.; Kukura, P.; Mathies, R. A.; Garavelli, M.; Cerullo, G. Conical Intersection Dynamics of the Primary Photoisomerization Event in Vision. *Nature* **2010**, *467*, 440.

(7) Virshup, A. M.; Chen, J.; Martínez, T. J. Nonlinear Dimensionality Reduction for Nonadiabatic Dynamics: The Influence of Conical Intersection Topography on Population Transfer Rates. *J. Chem. Phys.* **2012**, *137*, 22A519.

(8) Gozem, S.; Melaccio, F.; Valentini, A.; Filatov, M.; Huix-Rotllant, M.; Ferré, N.; Frutos, L. M.; Angeli, C.; Krylov, A. I.; Granovsky, A. A.; Lindh, R.; Olivucci, M. Shape of Multireference, Equation-of-Motion Coupled-Cluster, and Density Functional Theory Potential Energy Surfaces at a Conical Intersection. *J. Chem. Theory Comput.* **2014**, *10*, 3074.

(9) Levine, B. G.; Ko, C.; Quenneville, J.; Martínez, T. J. Conical Intersections and Double Excitations in Time-Dependent Density Functional Theory. *Mol. Phys.* **2006**, *104*, 1039.

(10) Yarkony, D. R. Diabolical conical intersections. *Rev. Mod. Phys.* **1996**, *68*, 985.

(11) Schirmer, J. Beyond the Random-Phase Approximation: A New Approximation Scheme for the Polarization Propagator. *Phys. Rev. A: At., Mol., Opt. Phys.* **1982**, *26*, 2395.

(12) Trofimov, A. B.; Schirmer, J. An Efficient Polarization Propagator Approach to Valence Electron Excitation Spectra. *J. Phys. B: At., Mol. Opt. Phys.* **1995**, *28*, 2299.

(13) Christiansen, O.; Koch, H.; Jørgensen, P. The Second-Order Approximate Coupled Cluster Singles and Doubles Model CC2. *Chem. Phys. Lett.* **1995**, *243*, 409.

(14) Head-Gordon, M.; Oumi, M.; Maurice, D. Quasidegenerate Second-Order Perturbation Corrections to Single-Excitation Configuration Interaction. *Mol. Phys.* **1999**, *96*, 593.

(15) Schirmer, J.; Trofimov, A. B. Intermediate State Representation Approach to Physical Properties of Electronically Excited Molecules. *J. Chem. Phys.* **2004**, *120*, 11449.

(16) Hättig, C. Structure Optimizations for Excited States with Correlated Second-Order Methods. *Adv. Quantum Chem.* **2005**, *50*, 37.

(17) Dreuw, A.; Head-Gordon, M. Single-Reference ab Initio Methods for the Calculation of Excited States of Large Molecules. *Chem. Rev.* **2005**, *105*, 4009.

(18) Starcke, J. H.; Wormit, M.; Dreuw, A. Unrestricted Algebraic Diagrammatic Construction Scheme of Second Order for the Calculation of Excited States of Medium-Sized and Large Molecules. *J. Chem. Phys.* **2009**, *130*, 024104.

(19) Dutoi, A. D.; Cederbaum, L. S.; Wormit, M.; Starcke, J. H.; Dreuw, A. Tracing Molecular Electronic Excitation Dynamics in Real Time and Space. *J. Chem. Phys.* **2010**, *132*, 144302.

(20) Laikov, D.; Matsika, S. Inclusion of Second-Order Correlation Effects for the Ground and Singly-Excited States Suitable for the Study of Conical Intersections: The CIS(2) Model. *Chem. Phys. Lett.* **2007**, *448*, 132.

(21) Send, R.; Furche, F. First-Order Nonadiabatic Couplings from Time-Dependent Hybrid Density Functional Response Theory:

DOI: 10.1021/acs.jpclett.9b00981
J. Phys. Chem. Lett. 2019, 10, 3426−3432

Consistent Formalism, Implementation, and Performance. *J. Chem. Phys.* **2010**, *132*, 044107.
(22) Shu, Y.; Parker, K. A.; Truhlar, D. G. Dual-Functional Tamm−Dancoff Approximation: A Convenient Density Functional Method that Correctly Describes S_1/S_2 Conical Intersections. *J. Phys. Chem. Lett.* **2017**, *8*, 2107.
(23) Li, S. L.; Marenich, A. V.; Xu, X.; Truhlar, D. G. Configuration Interaction-Corrected Tamm−Dancoff Approximation: A Time-Dependent Density Functional Method with the Correct Dimensionality of Conical Intersections. *J. Phys. Chem. Lett.* **2014**, *5*, 322.
(24) Grimme, S.; Waletzke, M. A Combination of Kohn−Sham Density Functional Theory and Multi-Reference Configuration Interaction Methods. *J. Chem. Phys.* **1999**, *111*, 5645.
(25) Kraka, E. Homolytic Dissociation Energies from GVB-LSDC Calculations. *Chem. Phys.* **1992**, *161*, 149.
(26) Gräfenstein, J.; Cremer, K. Development of a CAS-DFT Method Covering Non-Dynamical and Dynamical Electron Correlation in a Balanced Way. *Mol. Phys.* **2005**, *103*, 279.
(27) Filatov, M.; Liu, F.; Martínez, T. J. Analytical Derivatives of the Individual State Energies in Ensemble Density Functional Theory Method. I. General Formalism. *J. Chem. Phys.* **2017**, *147*, 034113.
(28) Kowalczyk, T.; Tsuchimochi, T.; Chen, P.-T.; Top, L.; Van Voorhis, T. Excitation Energies and Stokes Shifts from a Restricted Open-Shell Kohn−Sham Approach. *J. Chem. Phys.* **2013**, *138*, 164101.
(29) Kaduk, B.; Van Voorhis, T. Communication: Conical Intersections Using Constrained Density Functional Theory — Configuration Interaction. *J. Chem. Phys.* **2010**, *133*, 061102.
(30) Evangelista, F. A.; Shushkov, P.; Tully, J. C. Orthogonality Constrained Density Functional Theory for Electronic Excited States. *J. Phys. Chem. A* **2013**, *117*, 7378−7392.
(31) Maitra, N. T.; Zhang, F.; Cave, R. J.; Burke, K. Double Excitations within Time-Dependent Density Functional Theory Linear Response. *J. Chem. Phys.* **2004**, *120*, 5932.
(32) Cave, R. J.; Zhang, F.; Maitra, N. T.; Burke, K. A Dressed TDDFT Treatment of the 2^1A_g States of Butadiene and Hexatriene. *Chem. Phys. Lett.* **2004**, *389*, 39.
(33) Gagliardi, L.; Truhlar, D. G.; Li Manni, G.; Carlson, R. K.; Hoyer, C. E.; Bao, J. L. Multiconfiguration Pair-Density Functional Theory: A New Way To Treat Strongly Correlated Systems. *Acc. Chem. Res.* **2017**, *50*, 66.
(34) Berry, M. V. Quantal Phase Factors Accompanying Adiabatic Changes. *Proc. R. Soc. London, Ser. A* **1984**, *392*, 45.
(35) Herzberg, G.; Longuet-Higgins, H. C. Intersection of Potential Energy Surfaces in Polyatomic Molecules. *Discuss. Faraday Soc.* **1963**, *35*, 77.
(36) Gilbert, A. T. B.; Besley, N. A.; Gill, P. M. W. Self-Consistent Field Calculations of Excited States Using the Maximum Overlap Method (MOM). *J. Phys. Chem. A* **2008**, *112*, 13164.
(37) Helgaker, T.; Jørgensen, P.; Olsen, J. *Molecular Electronic-Structure Theory*; Wiley, 2000.
(38) Slavíček, P.; Martínez, T. J. Ab Initio Floating Occupation Molecular Orbital-Complete Active Space Configuration Interaction: An Efficient Approximation to CASSCF. *J. Chem. Phys.* **2010**, *132*, 234102.
(39) Shu, Y.; Hohenstein, E. G.; Levine, B. G. Configuration Interaction Singles Natural Orbitals: An Orbital Basis for an Efficient and Size Intensive Multireference Description of Electronic Excited States. *J. Chem. Phys.* **2015**, *142*, 024102.
(40) Liu, X.; Subotnik, J. E. The Variationally Orbital-Adapted Configuration Interaction Singles (VOA-CIS) Approach to Electronically Excited States. *J. Chem. Theory Comput.* **2014**, *10*, 1004.
(41) Subotnik, J. E. Communication: Configuration Interaction Singles Has a Large Systematic Bias against Charge-Transfer States. *J. Chem. Phys.* **2011**, *135*, 071104.
(42) Schreiber, M.; Silva-Junior, M. R.; Sauer, S. P. A.; Thiel, W. Benchmarks for Electronically Excited States: CASPT2, CC2, CCSD, and CC3. *J. Chem. Phys.* **2008**, *128*, 134110.
(43) Marques, M.; Gross, E. Time-Dependent Density Functional Theory. *Annu. Rev. Phys. Chem.* **2004**, *55*, 427.
(44) Furche, F. On the Density Matrix Approach to Time-Dependent Density Functional Response Theory. *J. Chem. Phys.* **2001**, *114*, 5982.
(45) Hirata, S.; Head-Gordon, M. Time-Dependent Density Functional Theory within the Tamm−Dancoff Approximation. *Chem. Phys. Lett.* **1999**, *314*, 291.
(46) Ben-Nun, M.; Martínez, T. J. Ab Initio Molecular Dynamics Study of Cis-Trans Photoisomerization in Ethylene. *Chem. Phys. Lett.* **1998**, *298*, 57.

DOI: 10.1021/acs.jpclett.9b00981
J. Phys. Chem. Lett. 2019, 10, 3426−3432